Applied Catalysis B: Environmental 84 (2008) 30–41

Contents lists available at ScienceDirect

Applied Catalysis B: Environmental

journal homepage: www.elsevier.com/locate/apcatb

Catalytic wet-air oxidation of aqueous solutions of formic acid, acetic acid and phenol in a continuous-flow trickle-bed reactor over Ru/TiO_2 catalysts

Albin Pintar *, Jurka Batista, Tatjana Tišler

National Institute of Chemistry, Hajdrihova 19, P.O. Box 660, SI-1001 Ljubljana, Slovenia

ARTICLE INFO

Article history:
Received 21 December 2007
Received in revised form 26 February 2008
Accepted 3 March 2008
Available online 18 March 2008

Keywords:
Acute toxicity tests
Catalytic wet-air oxidation
Heterogeneous catalysis
Ruthenium catalysts
Titanium oxide
Trickle-bed reactor
Wastewater treatment

ABSTRACT

Catalytic wet-air oxidation of aqueous solutions of formic acid, acetic acid and phenol was carried out in a trickle-bed reactor at $T = 328–523$ K and total pressures up to 50 bar over various Ru/TiO_2 catalysts. Complete oxidation of formic acid was obtained at mild operating conditions, and no catalyst deactivation occurred that could be attributed to the dissolution of active ingredient material. It was observed that besides oxidation route thermal decomposition contributes significantly to the removal of formic acid; Ru/TiO_2 catalysts could be thus efficiently used for transformation of HCOOH to H_2 and CO_2 in an inert atmosphere. Liquid-phase oxidation of acetic acid was found to be structure sensitive; the highest catalyst activity was obtained, when Ru phase on the catalyst surface prevailed in zero-valent state. Due to simultaneous oxidation of metallic Ru to RuO_2 during the reaction course, correspondingly lower conversion of acetic acid was measured in the reactor outlet. The employed Ru/TiO_2 catalysts enable complete removal of phenol and TOC at temperatures above 483 K; at these conditions, no carbonaceous deposits were accumulated on the catalyst surface. Apparent catalyst deactivation observed at temperatures below 463 K is attributed to strong adsorption of partially oxidized intermediates on the catalyst surface, which can be avoided by conducting the CWAO process at sufficiently high temperatures. The acute toxicity to *Daphnia magna* and *Vibrio fischeri* of end-product solutions compared with that of the feed solutions was significantly reduced by oxidative treatment over Ru/TiO_2 catalysts.

1. Introduction

Considering the need for environmental protection, one of the promising options for removal of toxic and non-biodegradable organic compounds from industrial wastewaters is destruction of these contaminants by catalytic wet-air oxidation (CWAO) [1]. In the CWAO process, the organic pollutants are oxidized by activated O_2 species in the presence of a solid catalyst, usually at temperatures of 403–523 K and pressures of 10–50 bar, into biodegradable intermediate products or mineralized into CO_2, water and associated inorganic salts. The CWAO of various organic compounds has been studied over metal oxides, mixed metal oxide systems, cerium-based composite oxides and supported noble metal catalysts [2]. From the economical point of view, there is still a need to improve catalytic activity and long-term stability of heterogeneous catalysts in order to achieve effective oxidative degradation of organic pollutants at temperatures and pressures as low as possible [3–5].

Titania and zirconia supported ruthenium catalysts have received much attention recently, because they exhibited high activity and chemical resistance in CWAO of different model pollutants [6–13] and industrial wastewaters [14,15]. The textures of ZrO_2 and TiO_2 supports [14] as well as the preparation parameters of the catalysts [13] affect the catalytic performances of Ru/TiO_2 and Ru/ZrO_2. The (initial) activity of ruthenium for CWAO of organic pollutants is quite sensitive: (i) to the oxidation–reduction treatment of supported ruthenium catalysts [7], (ii) to the oxidizing atmosphere at CWAO conditions [7,8,16], (iii) to the presence of suspended solids in effluents [15], and (iv) to deposition of carbonaceous species on the catalyst surface [17]. Moderate loss of catalytic activity at the start of reaction due to partial oxidation of the surface or subsurface of Ru particles has been reported for CWAO of *p*-hydroxybenzoic acid in batch and continuous-flow reactors [16].

Acetic acid is a refractory intermediate typically produced in the oxidation route of various organic oxygenated compounds including phenol [18,19]. During the wet-air oxidation of phenol in a continuous-flow bubble-column reactor packed with a pelletized $Ru/ZrO_2–TiO_2$ catalyst, maleic acid, acetic acid and formic acid were identified as the main reaction intermediates [17]. Supported

* Corresponding author. Tel.: +386 1 4760283; fax: +386 1 4760300.
E-mail address: albin.pintar@ki.si (A. Pintar).

0926-3373/$ – see front matter © 2008 Elsevier B.V. All rights reserved.
doi:10.1016/j.apcatb.2008.03.001

Ru catalysts exhibit good activity for the wet-air oxidation of acetic acid to carbon dioxide [6–8,19–21]; metallic ruthenium is more active than RuO_2 [20]. It is not necessary to attain complete oxidative degradation of acetic acid in the CWAO treatment of concentrated waste streams. When a low amount of this biodegradable intermediate is formed in the CWAO process, it can be efficiently removed by subsequent biological treatment. There is an increasing interest in the use of an integrated CWAO-biological process for the elimination of organic compounds in wastewater streams from the chemical manufacturing industries, because this process exhibits high potential to be used in closed-loop operation by recycling and reusing waters.

In this work, Ru(x wt.%)/TiO_2 catalysts (x = 1.5 and 3.0) were prepared by incipient-wetness impregnation method and tested for CWAO of aliphatic and aromatic model compounds, i.e. formic acid, acetic acid and phenol, in O_2-rich and He environments in a continuous-flow trickle-bed reactor. CWAO of formic acid was investigated in this study, because little information regarding the oxidation of this compound is available in the literature. On the other hand, CWAO of phenol aqueous solutions was carried out to investigate a potential of employed catalysts for effective (i.e. long-term) removal of the parent molecule and intermediates from the liquid phase, with a noticeable accumulation of carbonaceous species on the catalyst surface. With the aim of clarifying the relationship between the modification of active Ru phase under CWAO operating conditions and catalytic properties of Ru/TiO_2 catalysts, we examined the influence of reaction temperature, nature of oxidizing agent and ruthenium loading on the pollutant and total organic carbon (TOC) conversions. Behavior of catalysts before and after CWAO runs was comparatively investigated by means of XRD, TC, ICP-AES, TPR/TPO and textural measurements. The acute toxicity to *Daphnia magna* and *Vibrio fischeri* of feed and treated solutions, given as global efficiencies of Ru/TiO_2 catalysts for degradation and detoxification of model pollutants in water, are also reported.

2. Experimental

2.1. Catalyst preparation

The catalyst samples containing 1.5 and 3.0 wt.% of Ru were prepared by incipient-wetness impregnation of TiO_2 extrudates (Degussa-Hüls AG, Aerolyst type, d_p: 1.4 mm, S_{BET}: 51 m^2/g, V_{pore}: 0.36 cm^3/g, d_{pore}: 28 nm) with an aqueous solution of $RuCl_3 \cdot xH_2O$ (Acros Organics), whose concentration was accurately determined by ICP-AES before impregnation. The TiO_2 support was dried at 373 K in an oven for 2 h and then impregnated at room temperature with an appropriate volume of solution containing the Ru salt to obtain 1.5 and 3.0 wt.% Ru contents, respectively. After the impregnation step, the catalyst precursors were dried (overnight at room temperature, then at 313 K for 5 h, and finally at 378 K for 2 h) and reduced directly in H_2 flow of 250 ml/min at 573 K for 1 h without previous calcination. The reduced samples were cooled down to room temperature under N_2 flow. Reduction conditions were determined in this work by TPR analysis of dried catalyst precursors.

2.2. Catalyst characterization

The specific surface area, total pore volume and average pore width of the support and catalysts were determined from the adsorption and desorption isotherms of N_2 at 77 K using a Micromeritics ASAP 2020 instrument. This characterization was carried out after degassing of samples to 4 μm Hg for 1 h at 363 K and 2 h at 573 K. The same apparatus was used to perform static H_2 chemisorption analyses following the procedure described by Shen et al. [22]. Temperature-programmed reduction (H_2-TPR) and TPR-1/TPO/TPR-2 cycling measurements were performed with a Micromeritics Autochem II 2920 catalyst characterization system.

Before starting TPR runs, dried Ru catalyst precursors (0.15 g) were degassed under flowing Ar (50 ml/min) at 378 K for 30 min. After that, the samples were cooled to 233 K in Ar flow. A TPR was then performed under H_2(5 vol.%)/Ar flow (50 ml/min) at a heating rate of 5 K/min up to 773 K. The effluent gas was passed through a LN_2/iPA trap into the thermal conductivity detector. The TiO_2 support (0.25 g) was activated (90 min at 773 K in O_2(10 vol.%)/He flow), cooled to 273 K in O_2(10 vol.%)/He flow, and purged in flowing He (to remove the residual O_2) prior to performing TPR.

To verify whether the reducing–oxidizing treatments of fresh Ru(1.5 wt.%)/TiO_2 and Ru(3.0 wt.%)/TiO_2 samples have an influence on the catalyst surface properties and consequently on the catalytic activity and selectivity, comparative TPR-1/TPO/TPR-2 measurements were carried out for catalyst precursors reduced and oxidized at conditions similar to those used in the CWAO testing experiments. The temperature-programmed oxidation (TPO) experiments were performed following H_2-TPR (5 K/min up to 573 K) and purging (1 h at 598 K) the reduced samples with Ar to remove the residual H_2 and further cooling to 233 K. After that TPO runs were carried under O_2(10 vol.%)/He flow (50 ml/min) at a heating rate of 5 K/min up to 573 K. Then the re-oxidized samples were purged in He flow (1 h at 598 K) to remove the residual O_2, cooled to 233 K and then the second reduction run (TPR-2) was performed under the same conditions as the first run.

XRD patterns of fresh and used catalyst samples were obtained on a PANalytical X'Pert PRO diffractometer using Cu Kα radiation (λ = 0.15406 nm). Data were collected from 20 to 80° 2θ, at 0.034° and 100 s per step. Crystalline phases were identified by comparison with PDF standards from the International Centre for Diffraction Data (ICDD).

The high resolution electron micrographs of catalyst samples were recorded on a FE-SEM SUPRA 35VP (Carl Zeiss) microscope equipped with an EDAX energy dispersive X-ray spectrometer Inca 400 (Oxford Instruments).

The carbon content of carbonaceous deposits accumulated on the titania and catalyst surface during the reaction course was determined, after washing, and drying the spent support and catalysts, using a boat sampling module (Rosemount/Dohrmann, model 183) connected to a TOC analyzer (Rosemount/Dohrmann, model DC-190). Deposition of Fe on the catalyst during the CWAO reaction in dependence of the reactor material was verified by ICP-AES analysis of spent catalysts. Leaching of Ru and Ti from catalysts during the CWAO reaction was verified by ICP-AES analysis of collected liquid-phase samples.

2.3. CWAO experiments

CWAO experiments were carried out in a Microactivity-Reference unit (PID Eng&Tech, Spain), which is an automated and computer-controlled, continuous-flow trickle-bed reactor for catalytic microactivity tests. The properties of the catalyst bed and operating conditions are listed in Table 1. Concentrations of feed aqueous solutions were 2.0 g/l for formic acid (100%, Merck) and acetic acid (99–100%, Merck), and 1.0 g/l for phenol (99%, Aldrich). A fixed-bed tubular reactor (Autoclave Engineers) was made of a 305 mm o.d. × 9 mm i.d. stainless-steel (316-L) or Hastelloy C-276 (runs #6–11) tube that was heated with a reactor furnace and integrated within the hot box. Liquid and gaseous flows were introduced into the hot box system that includes an electric forced convection heater which permits the process route to be preheated and kept at temperatures up to 463 K. The liquid reactant was

Table 1
Experimental conditions of the catalytic wet-air oxidation of various organic compounds in a trickle-bed reactor

Mass of catalyst in bed (g)	3.0
Bed density (g cm^{-3})	0.94
Bed porosity (/)	0.41
Equivalent catalyst particle diameter (mm)	1.42
Catalyst particle density (g cm^{-3})	1.59
Reaction temperature (K)	328–523
Total operating pressure (bar)	10.2–49.7
Oxygen partial pressure (bar)	0–10.0
Gas flow rate (ml/min)	100
Superficial gas flow rate (kg m^{-2} s^{-1})	0.33–1.05
Liquid flow rate (ml/min)	0.6–1.8
Superficial liquid flow rate (kg m^{-2} s^{-1})	0.16–0.50
LHSV (h^{-1})	11.3–33.9

introduced into the unit using a HPLC positive alternative displacement pump (Gilson, model 307). The oxygen source in these experiments was pure O_2 (purity 5.0, Messer), which was fed to the system through an electronic HI-TEC mass-flow controller (Bronkhorst, model EL-FLOW). The preheated gas and liquid streams merge in a T-joint and are then introduced to the top of the reactor through a 10 μm sintered stainless-steel (316) filter (another is located at the outlet of the reactor, which protected the arrangement from possible finely separated catalyst fines). A porous (2 μm) plate made of Hastelloy C-276, supported on a 316 stainless-steel pipe, was placed inside near the middle of the reactor tube to support the fixed bed composed of 3.0 g of either TiO_2 extrudates or Ru/TiO_2 catalyst. The reaction temperature was measured by a K-type thermocouple, which was inserted through the upper end of reactor and was in contact with the catalyst bed, and regulated within ±1.0 K from the pre-set temperature by a PID temperature controller (TOHO, model TTM-005). The gas and liquid phases, which passed the catalytic bed in a co-current downflow mode and flowed out at the bottom of the reactor, were separated in a high-pressure liquid–gas (L/G) separator cooled with a Peltier cell. The L/G separator equipped with a micrometric servo-controlled valve and capacitive level sensor provides an efficient liquid discharge from the unit. The gas stream from the L/G separator was discharged through a second micrometric servo-controlled regulating valve, which was employed to provide continuous and constant flow of gases at the outlet (i.e. pressure control). In the off-gas stream, production of CO_2 and eventual formation of CO were monitored by a non-dispersive IR detector (Rosemount, model BINOS 1001).

2.4. Analysis of end-product solutions (TOC, HPLC) and acute toxicity tests

Representative liquid-phase samples, which were continuously collected from the L/G condenser/separator during the CWAO experiments, were analyzed for organic acids by HPLC using a 250 mm × 4.6 mm Synergi 4 μ Hydro-RP column thermostated at 295 K (UV detection at λ = 220 nm with a mobile phase of 0.020 M KH_2PO_4 with pH 2.9 at a flow rate of 0.7 ml/min). Identifications and quantifications of organic acids were obtained by comparison with internal standards. Phenol concentration was determined by isocratic HPLC analysis using a 150 mm × 4.6 mm Spherisorb ODS2 5 μ column thermostated at 295 K (UV detection at λ = 270 nm with a mobile phase of acetonitrile (50%) and DI water (50%) at a flow rate of 0.5 ml/min). The total amount of organic substances in aqueous-phase samples was determined by measuring total organic carbon by a Rosemount/Dohrmann DC-190 TOC analyzer. In all analyses, 3–4 repeated measurements were taken for each liquid sample, and the average value of TOC was reported. The error of analysis was never greater than ±0.5%.

The acute toxicity test with the freeze-dried bacteria *V. fischeri* NRRL-B-11177 obtained from the manufacturer (Dr. Lange GmbH, Düsseldorf, Germany) was performed according to the ISO standard [23]. The luminescence was measured on a LUMIStox 300 luminometer. The luminescent bacteria were exposed to different concentrations of feed sample and treated samples for 30 min at 288 ± 0.2 K and the percentage of inhibition was calculated for each concentration relative to the control. In each experiment eight concentrations and a control in two replicates were tested. The 30-min EC_{50} values with corresponding 95% confidence limits were calculated using a standard log-linear model supported by computer software [24].

D. magna Straus 1820 obtained from the Institut für Wasser, Boden und Lufthygiene des Umweltbundesamtes (Berlin, Germany) were cultured in a temperature-controlled room at 294 ± 1 K in 3-l aquariums covered with glass plates containing 2.5 l of modified M4 medium [25], illuminated with fluorescent bulbs (approximately 1800 lux) for 12 h per day. They were fed daily a diet of the green alga *Desmodesmus subspicatus* Chodat 1926 corresponding to 0.13 mg carbon/daphnia. One day before the start of the experiments reproductive daphnids were isolated and young neonates (aged about 24 h) were used. In the acute toxicity tests, daphnids were exposed to different concentrations of feed sample and treated samples and the immobile daphnids were counted after the 24 and 48 h of exposure [26]. In each definitive toxicity experiment five concentrations and a control in two replicates were tested. The 24-h and 48-h EC_{50} values with corresponding 95% confidence limits were obtained using probit analysis [27].

The bioassay concentrations, the end-product enhancement factors and detoxification factors were calculated using the procedure described in detail in previous studies [15,28]. Because of the wide disparity in model pollutants, and eventual complexity of end-product solutions obtained during the CWAO of phenol, a lumped parameter, i.e. TOC, was used in order to quantitatively evaluate the toxicity of initial and treated effluents by this method.

3. Results and discussion

3.1. Catalyst characterization

3.1.1. Fresh catalysts

Specific surface area, total pore volume and average pore width of the support and fresh catalysts (Table 2) show that deposition of 1.5–3.0 wt.% of Ru did not significantly modify the textural properties and the corresponding XRD powder patterns (not shown). The XRD pattern of TiO_2 support revealed the presence of anatase (titanium oxide, PDF 03-065-5714) and rutile (titanium oxide, PDF 00-004-0551) phases, and that anatase is the prevailing crystallographic form. The XRD patterns are not affected by the deposition of ruthenium, as the peak of metallic Ru is not observed for Ru(1.5 wt.%)/TiO_2 catalyst. Due to the close coincidence between the positions of ruthenium diffraction peaks (ruthenium, syn, PDF 06-0663: $2\theta = 38.39$, 42.15 and

Table 2
Specific surface area (S_{BET}), total pore volume (V_{pore}), average pore width (d_{pore}) and ruthenium dispersion (D_{Ru}) of fresh Ru/TiO_2 catalyst samples prepared by the incipient-wetness impregnation method and reduced directly in H_2 flow (1 h, 573 K) without previous calcination

Sample	S_{BET} (m^2/g)	V_{pore} (cm^3/g)	d_{pore} (Å)	D_{Ru} (%)
TiO_2	51	0.364	282	–
Ru(1.5 wt.%)/TiO_2	50	0.355	285	8.6
Ru(3.0 wt.%)/TiO_2	50	0.344	274	5.4

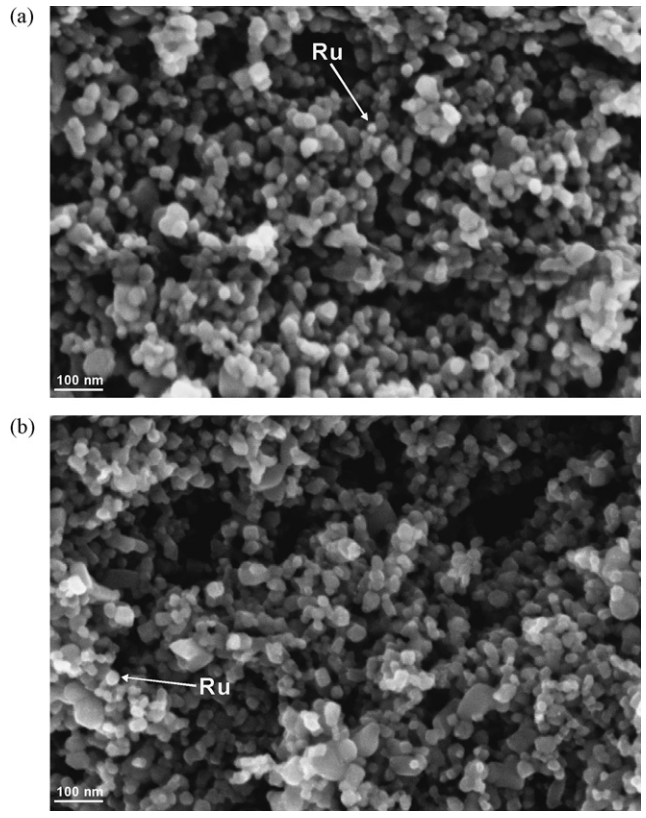

Fig. 1. SEM micrographs of fresh catalyst samples: (a) Ru(1.5 wt.%)/TiO_2; (b) Ru(3.0 wt.%)/TiO_2.

44.01°) and those corresponding to rutile, the ruthenium detection in Ru(3.0 wt.%)/TiO_2 catalyst was not possible by XRD analysis.

As indicated in Table 2, the accessibility of ruthenium is poor on both Ru(1.5 wt.%)/TiO_2 and Ru(3.0 wt.%)/TiO_2 catalysts. Low dispersion determined on catalysts after reduction at 573 K can be, at least partially, explained by an inhibiting effect of residual chloride on the fraction of Ru surface available for H_2 chemisorption [29–31] and the use of large-sized TiO_2 extrudates [14]. The presence of rather large and discrete Ru particles on the surface of synthesized catalysts, as determined by H_2 chemisorption measurements (15 and 25 nm for Ru loadings of 1.5 and 3.0 wt.%, respectively) is supported by SEM examination (Fig. 1), which reveals the presence of Ru clusters in the range of 10–20 nm (Ru(1.5 wt.%)/TiO_2) and 14–34 nm (Ru(3.0 wt.%)/TiO_2).

H_2-TPR profiles of catalyst precursors and TiO_2 support were determined in the temperature range from 233 to 773 K. At the employed reduction treatment, TPR profile of unloaded TiO_2 support (not shown) revealed that partial reduction of TiO_2 surface by H_2 starts close to 573 K. We observed color changes of the TiO_2 sample upon hydrogen exposition during TPR run, indicating the surface reduction of titanium dioxide (white) to TiO_x (pale blue-violet) [32,33]; after reduction at 773 K the value of x was found to be 1.995. The H_2-TPR profiles of Ru(1.5 wt.%)/TiO_2 and Ru(3.0 wt.%)/TiO_2 catalyst precursors exhibit peaks located between 273 and 473 K, and a weak and broad reduction peak in the temperature range from 523 to 623 K (see Fig. 2a and b). The detection of multiple hydrogen consumption peaks for both catalyst precursors suggests that more than one type of $RuCl_3$ species (i.e. atomically dispersed, micro-crystals) are present on the surface [29]. The temperatures of the peak maxima obtained within the range from 273 to 473 K are in good agreement with the

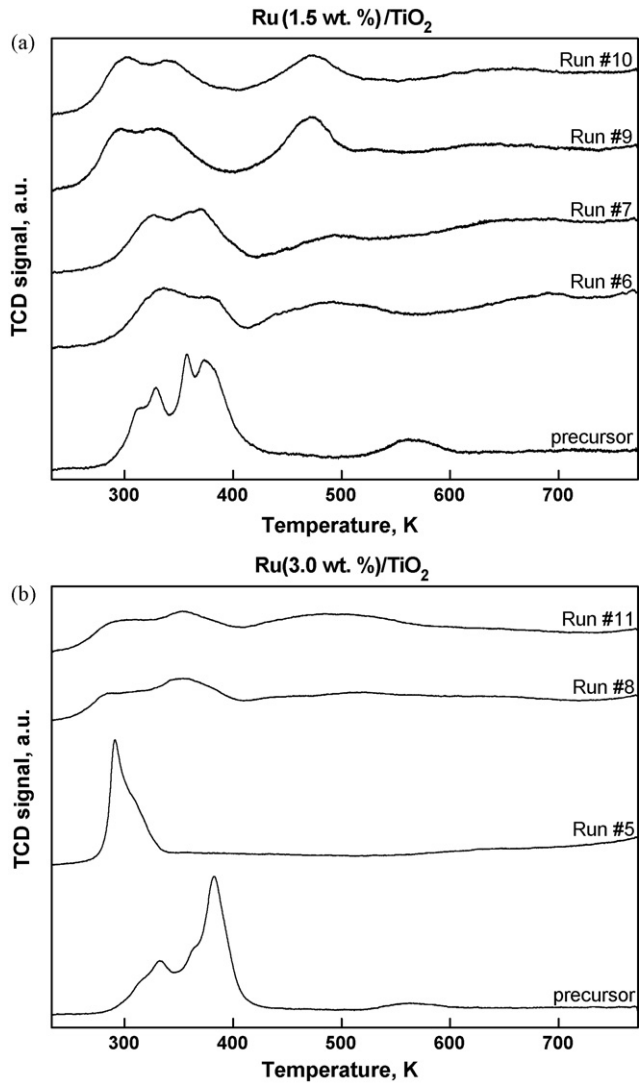

Fig. 2. TPR spectra of catalyst precursors and catalyst samples used in various WAO experiments: (a) Ru(1.5 wt.%)/TiO_2; (b) Ru(3.0 wt.%)/TiO_2.

results of TPR analysis of similar catalyst precursors [29]. It is evident from Fig. 2 that reduction of ruthenium ion species in the prepared catalyst precursors is enhanced because the temperatures of the peak maxima in these precursors are lower than those in the unsupported $RuCl_3 \cdot 2H_2O$ (i.e. two maxima at 475 and 485 K). The lower peak maximum temperatures probably reflect the state of dispersion of the supported $RuCl_3$ [29]. Further comparison of TPR profiles for prepared catalyst precursors (Fig. 2) and TiO_2 support provide an evidence that a small and broad band located above 523 K in TPR patterns of both precursors (T_{max} close to 563 K) can be attributed to partial reduction of titania surface, which is promoted by the presence of ruthenium particles (unloaded TiO_2 support: T_{max} close to 603 K). We cannot exclude that this reduction peak is partially associated with the reduction of a small amount of ruthenium oxide or oxychloride that may be formed by the exposition and drying of impregnated solids in air at 378 K [34,35].

The TPR-1/TPO/TPR-2 cycling of Ru/TiO_2 samples revealed that the TPR profile characteristics are not reproducible (not shown). TPO profiles of both catalysts show a broad peak in the temperature range from 233 to 573 K, assigned to the formation of RuO_2 in accordance with the H_2 uptake determined in the second TPR run. This run indicates a peak at T_{max} = 371 K for

Table 3
Textural and physicochemical properties of catalysts used in different CWAO runs

Catalyst	Run number	Model pollutant	S_{BET} (m^2/g)	V_{pore} (cm^3/g)	d_{pore} (Å)	TC (μg/g)	Fe (μg/g)
TiO_2[a]	3a	Phenol	n.d.[b]	n.d.	n.d.	104	n.d.
Ru(1.5 wt.%)/TiO_2	6	Acetic acid	40	0.339	342	159	1243
	7	Acetic acid	41	0.342	337	147	24
	9	Both acids	47	0.349	294	276	28
	10	Phenol	44	0.347	314	197	<10
Ru(3.0 wt.%)/TiO_2	5	Formic acid	54	0.345	255	3494[c]	<10
	8	Acetic acid	42	0.343	326	113	122
	11	Phenol	43	0.340	316	100	< 10

[a] TC of fresh TiO_2 support = 228 μg/g.
[b] Not determined.
[c] No rinsing of catalyst sample with distilled water was performed after the completion of experiment.

Ru(1.5 wt.%)/TiO_2 and split peaks (T_{max} = 369 and 401 K) for Ru(3.0 wt.%)/TiO_2. Both the TPR-2 peak areas (reduction of RuO_2) that are smaller than in the first TPR runs (reduction of $RuCl_3$), and the return of TCD signal to the initial value only in the case of TPR-2 runs reflect changes occurring during TPR/TPO treatment of Ru/TiO_2 samples in the temperature range from 233 to 573 K. No measurable reduction of the support promoted by the presence of Ru particles was observed under TPR-2 reducing conditions.

3.1.2. Catalysts after the CWAO runs

In order to elucidate an influence of reaction medium and reaction conditions (runs #5–11, Table 3) on the variation of Ru oxidation states, and eventual structural and textural modifications of catalysts (i.e. poisoning, sintering), XRD, H_2-TPR, N_2 adsorption–desorption isotherms (at 77 K), TC, and ICP-AES analyses were performed on catalysts before and after the CWAO runs (used catalyst samples were thoroughly washed with distilled water and dried prior to analysis). A comparison of X-ray powder diffraction patterns of spent Ru/TiO_2 catalysts to those of fresh catalysts reveals that no peak characteristic of metallic Ru, ruthenium oxide phases or other phases (i.e. Fe, Fe-oxides, carbon) was identified; the reflections correspond to those of the TiO_2 support (not shown). Results of H_2-TPR analysis of spent Ru/TiO_2 catalysts are presented in Fig. 2. As can be seen, H_2 uptake in spent catalysts appears in temperature ranges 273–415 and 423–573 K. In agreement with the TPR-1/TPO/TPR-2 results for fresh Ru/TiO_2 catalysts, a broad TPR peak in the temperature range from 273 to 415 K can be reasonably assigned to different rates of reduction of smaller and larger oxidized Ru particles [36]. Comparing the H_2 consumption measured in the temperature range from 273 to 423 K for each catalyst before and after CWAO run, we evaluated the portion of metallic Ru that undergoes oxidation under given reaction conditions (Table 1). We found out that about 22–30% of deposited Ru phase is partially oxidized during the CWAO runs (Fig. 2). Further, Ru dispersion in spent catalysts was found to be similar to values reported in Table 2, which confirms that in the applied range of operating conditions sintering of Ru particles does not occur to a measurable extent. Table 3 summarizes the textural properties of used catalysts and the amounts of carbon and Fe (arising from eventual corrosion of stainless-steel tubing in the hot box and reactor components) deposited on the surface of catalyst particles. The obtained values confirm that the undesirable formation of charred products on the catalyst surface, which could take place in parallel to oxidation reaction, was avoided.

3.2. Hydrodynamic considerations

Liquid hold-up, residence time of the liquid phase in the catalytic bed, and catalyst external wetting efficiency during CWAO runs were determined using a procedure described in detail in our previous study [15]. Given the experimental conditions listed in Table 1, all oxidation runs performed in this study were conducted in a low-interaction (LIR) trickle-flow regime (L was in the range of 0.16–0.50 kg m^{-2} s^{-1}), which means that the liquid trickles down the packing in the form of droplets, films and rivulets, while the continuous gas phase occupies the remaining porous space and flows separately [37,38]. At the employed operating conditions 9–17% of voids was occupied with the liquid phase, which is also in very good agreement with the liquid hold-up measurements of Goto and Smith [39]. It can be seen in Fig. 3a that the residence time of the liquid phase in the catalytic bed was in the range from 0.12 to 0.33 min. Analysis of the wetting

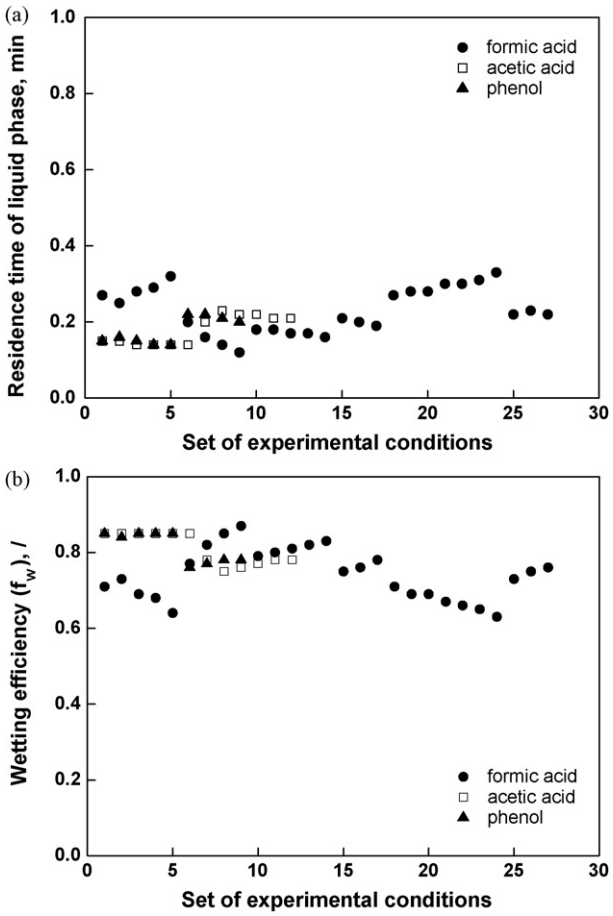

Fig. 3. Calculated values of residence time of liquid phase and wetting efficiency at various conditions of CWAO runs performed in this study.

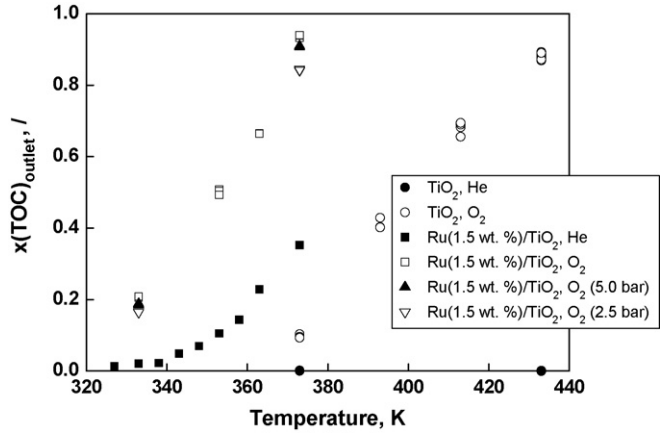

Fig. 4. TOC conversion as a function of temperature measured during formic acid oxidation in a trickle-bed reactor packed with different catalysts. $p(O_2)$: 10.0 bar, $\Phi_{vol,L}$: 0.6 ml/min, $c_{HCOOH,feed}$: 2.0 g/l.

efficiency (Fig. 3b) has shown that at the used operating conditions this parameter was in the range of 0.63–0.87, which implies that the external surface of catalyst particles was only partially wetted and thus directly exposed to the gas phase stream. The calculated values of wetting efficiency are in good agreement with the results of other investigations [37,40].

3.3. Catalytic activity and deactivation in CWAO reactions

3.3.1. CWAO of formic acid

Fig. 4 shows TOC conversions as a function of reaction temperatures obtained during the oxidation of formic acid in a trickle-bed reactor packed with the TiO_2 support or Ru(1.5 wt.%)/TiO_2 catalyst. In order to evaluate the contributions of both thermal and oxidative reaction routes in the decomposition of formic acid additional experiments were performed with He. A comparison of the TOC conversions obtained in He over the TiO_2 support and Ru(1.5 wt.%)/TiO_2 catalyst shows that formic acid decomposes by thermal degradation only in the presence of ruthenium catalyst. It is clearly evident that at our reaction conditions thermal degradation of formic acid over the bare TiO_2 support in He up to 433 K can be neglected (Fig. 4). The results in Fig. 4, obtained for bare TiO_2 support, show that oxidative degradation of formic acid starts at about 373 K (TOC conversion of ~10%) and leads to about 90% TOC conversion at 433 K. The Ru(1.5 wt.%)/TiO_2 considerably enhances the removal of formic acid; e.g., TOC conversion of ~20 and ~90% were obtained at 333 and 373 K, respectively (Fig. 4). Variation of O_2 partial pressure at a constant reaction temperature moderately affects the oxidation of formic acid. For instance, at a reaction temperature of 373 K, TOC conversion reduced from 95 to 85% when $p(O_2)$ decreased from 10.0 to 2.5 bar.

Fig. 5a shows TOC reduction as a function of reaction temperature measured during the treatment of formic acid in inert He atmosphere over Ru(3.0 wt.%)/TiO_2 catalyst. The catalyst considerably promotes thermal degradation of formic acid. Within an experimental error, constant TOC conversion as a function of time on stream (~80% at 398 K) was obtained in the period of 20 h (Fig. 5b). In runs depicted in Fig. 5, no carbon monoxide was detected in the off-gas stream; carbon dioxide was found to be the only gaseous product. This confirms that at the employed operating conditions formic acid is thermally decomposed to H_2 and CO_2 over titania-supported Ru catalyst. To conclude, the above results demonstrate that Ru/TiO_2 catalysts used in the present study have a potential for the production of H_2 and CO_2 from

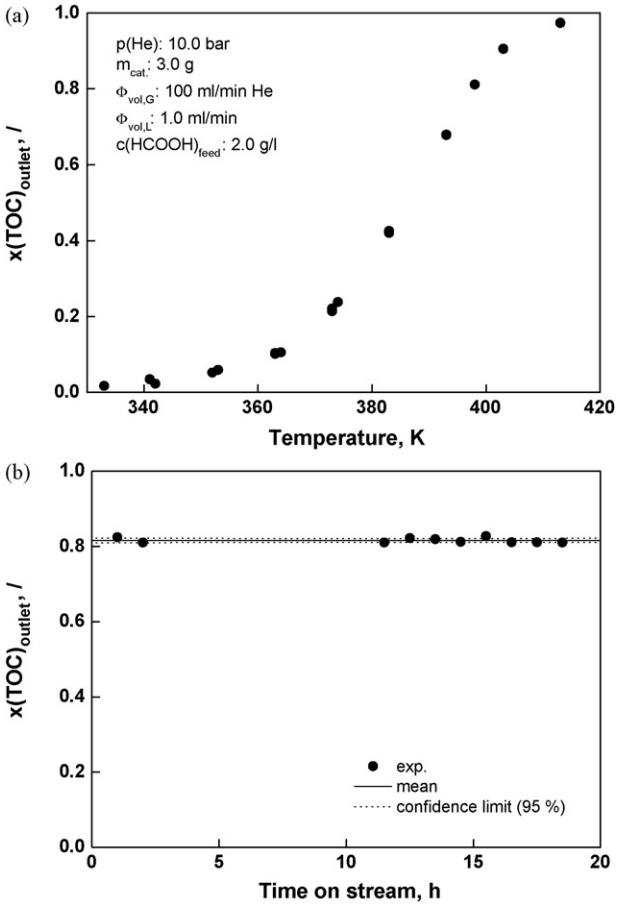

Fig. 5. (a) TOC conversion as a function of temperature measured during the treatment of formic acid in inert He atmosphere over Ru(3.0 wt.%)/TiO_2 catalyst; (b) TOC conversion as a function of time on stream at T = 398 K.

wastewaters or other solutions containing formic acid in significant quantities.

Fig. 6a illustrates dependence of TOC conversion on the residence time of the liquid phase obtained during the wet-air oxidation of formic acid over Ru(1.5 wt.%)/TiO_2 and Ru(3.0 wt.%)/TiO_2 catalysts at 373 K and $p(O_2)$ = 10.0 bar. The residence time was expressed as the ratio between the weight of catalyst ($m_{cat.}$) and the term $\Phi_{vol,L} \cdot c_{HCOOH,feed}$. At the given residence time, both catalysts give similar TOC conversions (about 95% when the liquid flow rate was set to 1.0 ml/min). Change in ruthenium loading slightly affects TOC conversion (Fig. 6a), which is attributed to the facts that thermal degradation of formic acid contributes to the overall TOC removal and that TOC conversion is influenced by mass-transfer limitations in the catalytic bed. Fig. 6b shows TOC conversion as a function of time on stream for oxidation runs carried out at various reaction temperatures over Ru/TiO_2 catalysts by using O_2 or air as oxidizing agents. Under net oxidizing conditions, $p(O_2)$ = 10.0 bar, complete TOC removal from the liquid phase was reached over both catalysts at 383 K. In addition, no decrease in TOC conversion with time on stream was observed in the period of 30 h. Switching to air (i.e. subsequent experiments) led to a decrease of the TOC conversion to ~75% (see Fig. 6b, air, 373 K). After further increasing the reaction temperature, the TOC conversion increased to ~98% at 413 K. Taking into account that in the investigated range of experimental conditions partial oxidation of ruthenium particles (26%) took place in the Ru(3.0 wt.%)/TiO_2 catalyst (see run #5 in Fig. 2b) and that no decrease of catalyst activity was observed with time on stream, it is reasonable to

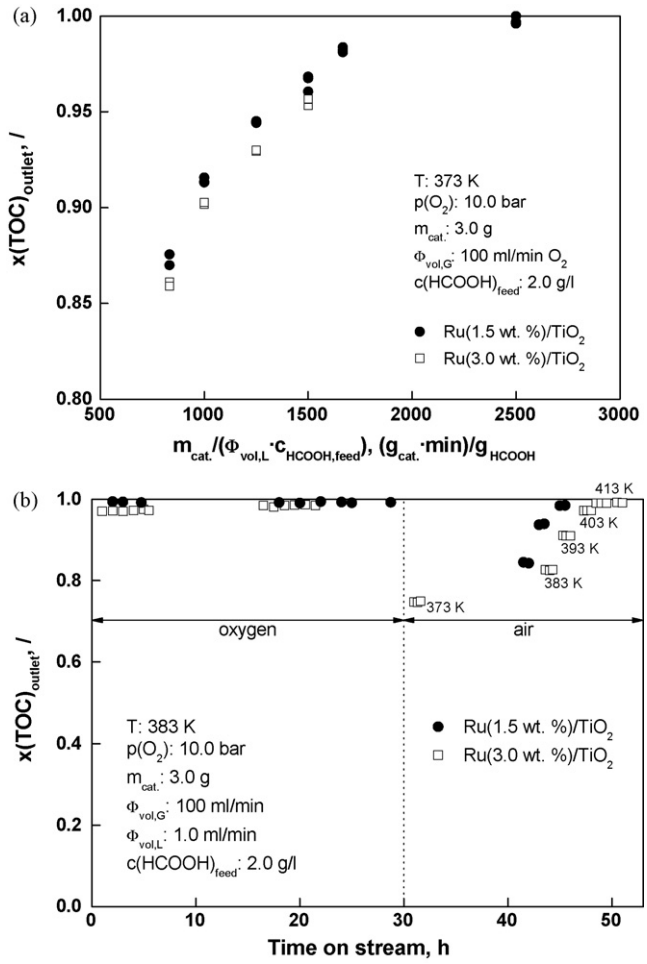

Fig. 6. (a) TOC conversion as a function of $m_{cat.}/(\Phi_{vol,L} \cdot c_{HCOOH,feed})$ ratio measured during formic acid oxidation over various Ru/TiO_2 catalysts; (b) TOC conversion as a function of time on stream measured at various temperatures by using different oxidizing agents.

conclude that both Ru^0 and RuO_2 phases are active in the TOC removal during WAO of formic acid (Figs. 4–6). Finally, results depicted in Fig. 6b confirm that no catalyst deactivation occurred which could be attributed to the dissolution of active ingredient material.

3.3.2. CWAO of acetic acid

An experiment performed over the TiO_2 support at $p(O_2) = 10.0$ bar and liquid flow rate of 0.6 ml/min in the temperature range from 413 to 483 K demonstrated that the bare TiO_2 support does not exhibit catalytic activity for acetic acid oxidation.

Fig. 7 shows TOC removal as a function of time on stream obtained during the oxidation of acetic acid at various reaction temperatures in the presence of Ru/TiO_2 catalysts. First of all, it should be mentioned that in any of runs depicted in Fig. 7 no formic acid was detected in the discharged liquid phase, which could be formed as an intermediate during CWAO of acetic acid. In order to elucidate the possible influence of the reactor material on the modification of catalyst properties and consequently the measured data, CWAO of acetic acid was conducted in reactor tubes made of stainless-steel 316-L (Fig. 7a, run #6) or Hastelloy C-276 (Fig. 7b, run #7) packed with a Ru(1.5 wt.%)/TiO_2 catalyst. A series of consecutive steps (I–VII) were performed to observe the effect of reaction temperature, flow rate of liquid phase (0.6 and 1.0 ml/min

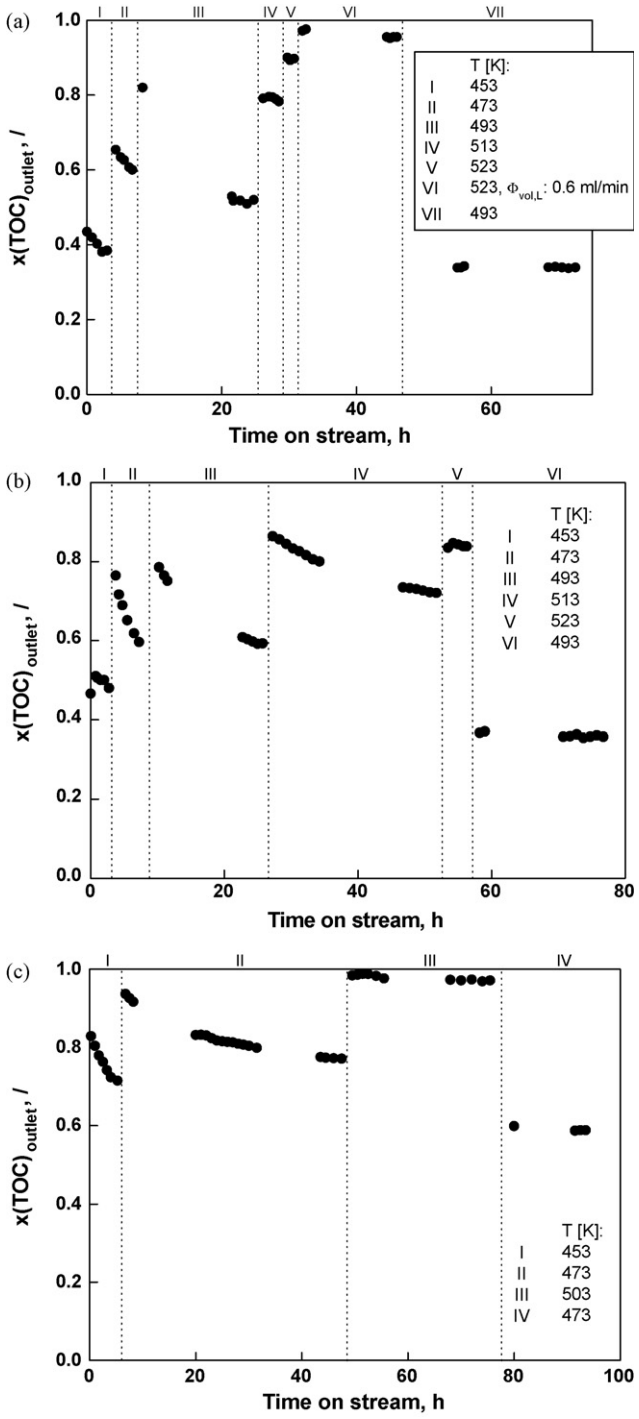

Fig. 7. TOC conversion as a function of time on stream measured during acetic acid oxidation at various reaction temperatures over: (a and b) Ru(1.5 wt.%)/TiO_2; (c) Ru(3.0 wt.%)/TiO_2 catalysts. $p(O_2)$: 10.0 bar, $\Phi_{vol,L}$: 1.0 ml/min, $c_{CH_3COOH,feed}$: 2.0 g/l.

for VI and all other steps, respectively) and partial pressure of oxygen (10.0 bar O_2 and 10.0 bar He for I–VII and transition step between VI and VII, respectively) on the level of residual TOC (Fig. 7a). It is evident that in the temperature range from 453 to 493 K the TOC conversion declines with time on stream at given reaction temperature (I–III). For instance, at 493 K the TOC conversion decreases from the initial value of ~82% at $t = 8$ h to ~48% at $t = 25$ h. An increase in TOC conversion with time on stream in consecutive steps was observed after each increase of reaction temperature (I–V) or retention time (Fig. 7a, compare

steps V and VI). Maximum TOC conversion of ~95% was obtained for $\Phi_{vol,L}$ = 0.6 ml/min at 523 K at t = 32 h (Fig. 7a, step VI). When the next consecutive step was performed under He at the same T and $\Phi_{vol,L}$ (transition between steps VI and VII, not shown in Fig. 7a), a sharp decrease in TOC conversion was observed (less than 5% conversion at t = 51 h). In further successive oxidation step (VII) that was performed at operating conditions identical to those of oxidation step III, the obtained TOC conversion was lower (~35%, t = 53–71 h) in comparison to that measured in step III (~48% at t = 25 h).

The TOC conversions obtained in the presented consecutive steps of run #6 (Fig. 7a) can be explained by taking into account changes of ruthenium oxidation states on the catalyst surface in dependence of reaction temperature. Comparing the H_2 consumption measured in the temperature range from 273 to 423 K for catalyst samples before and after CWAO run #6, we evaluated that about 26% of the metallic ruthenium undergoes oxidation under the reaction cycle presented in Fig. 7a. Since neglected amounts of carbon were deposited on the surface of used catalyst (Table 3), no leaching of Ru and Ti from Ru/TiO_2 catalysts (within the detection limits of 0.2 and 0.1 mg/l, respectively) was revealed under the given operating conditions (Table 1), and no structural changes were observed by XRD analysis (not shown), a decrease in TOC conversion with time on stream can be explained by assuming that partial oxidation of initially reduced catalyst occurred simultaneously to CWAO of acetic acid. During an increase of reaction temperature in next steps (Fig. 7a, II–V), the partially oxidized catalyst exhibited higher TOC conversions, simply due to higher temperatures applied. However, since no steady-state behavior regarding TOC conversion was obtained in any of the reaction steps (Fig. 7a), it can be concluded that oxidation of metallic Ru phase on the catalyst surface took place during the entire reaction course. This is particularly obvious by comparing TOC conversions in steps III and VII, conducted at identical operating conditions.

TOC conversion as a function of time on stream measured during acetic acid oxidation at various reaction temperatures in Hastelloy C-276 reactor tube (run #7) is depicted in Fig. 7b. During each step, a decrease in TOC conversion can be again observed with time on stream that is attributed to partial oxidation of metallic Ru phase on the catalyst surface. In step VI (493 K) the TOC conversion is very close to the one measured in step VII (run #6). In the last step, only slight decrease of TOC conversion was observed further with time on stream. A TPR analysis (Fig. 2a) revealed that similar amounts of ruthenium particles were oxidized under operating conditions applied in run #7 (30%) in comparison to run #6 (26%). As a consequence of different reactor material, higher deposition of Fe on the surface of Ru/TiO_2 catalyst was observed in the experiment conducted in the stainless-steel 316-L reactor tube (compare values for runs #6 and #7 in Table 3). However, since in both runs similar TOC conversion vs. time on stream dependencies were measured and very similar TOC conversions were obtained in final oxidation steps, it is believed that slightly higher amount of deposited Fe in run #6 has negligible effect on catalyst performance. Anyway, to avoid any influence of Fe loading on measured TOC data, the following CWAO experiments (runs #8–11) were carried out in a reactor made of Hastelloy C-276.

The above results indicate that starting the CWAO of acetic acid with a reduced catalyst leads to higher initial TOC conversion. However, due to partial oxidation of Ru^0 taking place in parallel to acetic acid oxidation a pronounced decrease of TOC conversion with time on stream is observed. This is because the process of surface oxidation is the fastest at the beginning of oxidation run. For a given composition of the reaction mixture, the amounts of RuO_2 and Ru^0 on the catalyst surface will depend on reaction temperature and concentration of liquid-dissolved oxygen. The highest temperature applied for the oxidation of acetic acid determines the maximum degree of oxidation of catalyst surface. Subsequent operation at lower temperatures has little impact on further oxidation of Ru particles, because after cooling almost steady-state TOC conversion is immediately observed (see, e.g., Fig. 7b, step VI).

Fig. 7c illustrates TOC conversion as a function of time on stream obtained during the CWAO of acetic acid in the presence of Ru(3.0 wt.%)/TiO_2 catalyst. In this experiment (run #8), four consecutive steps (I–IV) were performed to observe the effect of reaction temperature on TOC removal at the same $p(O_2)$ and $\Phi_{vol,L}$ as applied in run #7 over the Ru(1.5 wt.%)/TiO_2. A comparison of results illustrated in Fig. 7b and c shows that acetic acid was more easily oxidized in the presence of a catalyst with higher Ru loading. Maximum acetic acid conversion of ~95% was obtained at 503 K at time on stream of 78 h (Fig. 7c, step III). Since neglected amounts of carbon and Fe were determined on the surface of spent catalyst and no textural and structural changes were observed (see run #8 in Table 3), higher activity of Ru(3.0 wt.%)/TiO_2 catalyst can be explained by lower extent of oxidation of ruthenium particles on the catalyst surface. From TPR profiles of spent Ru/TiO_2 catalysts (Fig. 2), it follows that about 30 and 25% of metallic ruthenium undergoes oxidation during CWAO of acetic acid over Ru(1.5 wt.%)/TiO_2 and Ru(3.0 wt.%)/TiO_2 catalysts, respectively. Based on the above discussion, it can be concluded that liquid-phase oxidation of acetic acid is structure sensitive. The highest catalyst activity is measured at the beginning of oxidation run, when Ru phase on the catalyst surface prevails in zero-valent state. On the contrary to results of formic acid oxidation, the presence of RuO_2 phase on the catalyst surface decreases TOC removal during CWAO of acetic acid. These findings are in agreement with the results of Pham Minh et al., who investigated stability of Ru/TiO_2 and Ru/ZrO_2 catalysts during CWAO of *p*-hydroxybenzoic acid in batch and continuous-flow reactors [16].

Since H_2 is formed *in-situ* during the thermal decarboxylation of formic acid while passing the bed composed of Ru/TiO_2 particles, we proposed an idea that this could be used to improve CWAO of acetic acid by decreasing the extent of oxidation of surface Ru clusters. Correspondingly, an experiment was carried out in which the feed solution contained both carboxylic acids. TOC conversion as well as conversion of formic and acetic acids as a function of time on stream obtained during the CWAO of aqueous solution containing formic acid (1.0 g/l) and acetic acid (1.0 g/l) in the presence of Ru(1.5 wt.%)/TiO_2 catalyst under O_2 or He gas stream is presented in Fig. 8. An oxidation experiment (run #9) was carried out in seven consecutive steps by changing the reducing ($p(He)$ = 10.0 bar) and oxidizing ($p(O_2)$ = 10.0 bar) conditions in a cyclic way at T = 453 K. Analysis of liquid-phase samples by HPLC and off-gas stream by selective detectors (i.e. CO, CO_2) at any time on stream revealed complete conversion of formic acid either in He or O_2 atmosphere (see Fig. 8b). Irrespectively of the applied oxygen pressure, CO_2 without any trace of CO was detected, indicating complete decomposition of formic acid through decarboxylation under the chosen reaction conditions. Interestingly, using He partial pressure of 10.0 bar, conversion of acetic acid of about 25% was observed in the first step. One could assume that this is due to the reduction of partially oxidized ruthenium species or catalyst surface caused by partial oxidation of acetic acid under (He) reducing conditions (i.e. as TPR of RuO_x with acetic acid). However, this possibility should be ruled out because no acetic acid conversion was observed in subsequent reaction steps carried out in He atmosphere. It is more likely that the observed conversion of acetic acid in the presence of completely reduced Ru/TiO_2 catalyst is due to the decarboxylation of fed acetic acid stream to CO_2 and CH_4 (or H_2) promoted by metallic Ru [41,42];

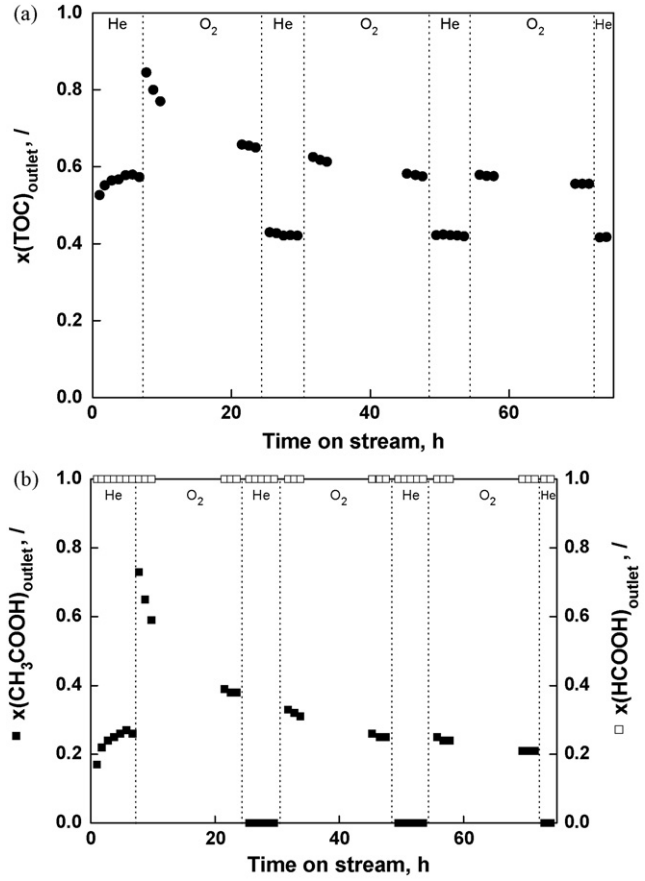

Fig. 8. TOC conversion (a) as well as conversion of formic and acetic acids (b) as a function of time on stream measured during CWAO of aqueous solution containing formic acid (1.0 g/l) and acetic acid (1.0 g/l) in a trickle-bed reactor packed with Ru(1.5 wt.%)/TiO_2 catalyst under oxygen or He gas stream. ***T***: 453 K, p(He or O_2): 10.0 bar, $\Phi_{vol,L}$: 1.0 ml/min.

this assumption remains subject of further investigation. Switching to O_2 led first to high conversion of acetic acid (~75% at t = 7 h), which then decreased to less than 40% (Fig. 8b) due to simultaneous oxidation of the catalyst surface. Switching back to the He stream, no conversion of acetic acid was observed; the measured TOC conversion in this step is attributed to complete transformation of formic acid (Fig. 8a). After switching back to O_2 (O_2 stream, steps IV and VI), conversion of acetic acid further decreased with time on stream (from ~35 to ~20% at 30 and 72 h, respectively), which can be explained by the progressive partial oxidation of metallic ruthenium particles (see Fig. 2a, run #9: ~30% RuO_2) that are initially very active for the oxidation of acetic acid. Under reducing (He) conditions, H_2 formed during the decarboxylation of formic acid probably due to too low concentration in the liquid phase does not affect the extent of partial reduction of RuO_2 layer, since the conversion of acetic acid remains unchanged and equal to 0% after each He–O_2 cycle and gradually decreases in each subsequent oxidation step.

3.3.3. CWAO of phenol

Fig. 9a presents TOC conversion vs. reaction temperature dependencies obtained during the oxidation of aqueous phenol solution (1.0 g/l) in the presence of bare TiO_2 support. The support exhibited catalytic activity under oxidizing conditions at temperatures higher than 433 K (i.e. ~40% TOC removal at 513 K). Examination of the support after reaction under oxidative conditions by XRD and TC analyses showed that the TiO_2 support

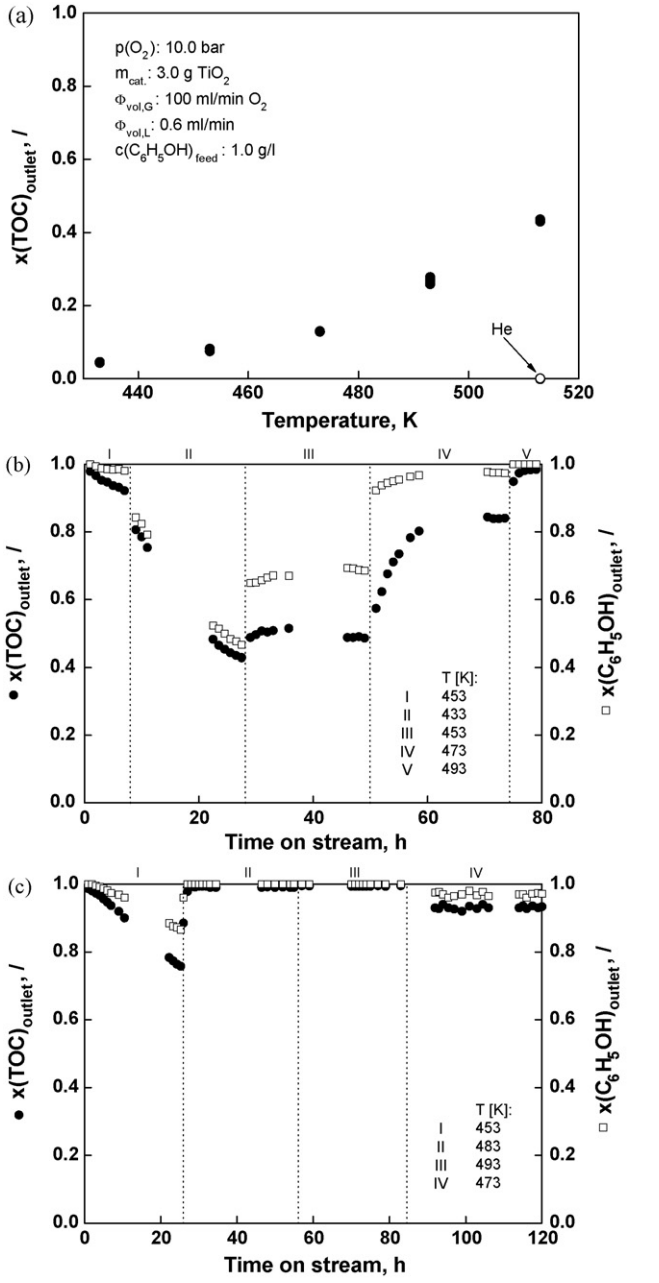

Fig. 9. (a) TOC conversion as a function of temperature measured during liquid-phase phenol oxidation in the presence of bare TiO_2 support; phenol and TOC conversion as a function of time on stream obtained over (b) Ru(1.5 wt.%)/TiO_2 and (c) Ru(3.0 wt.%)/TiO_2 catalysts. p(O_2): 10.0 bar, $\Phi_{vol,L}$: 1.0 ml/min, $c_{C_6H_5OH,feed}$: 1.0 g/l.

was not modified and that carbonaceous deposits were not accumulated on the support surface (Table 3: 228 and 104 μg TC/g_{solid} for fresh and used TiO_2 support, respectively). Under He, there was no removal of organic carbon from the liquid phase (Fig. 9a).

Figs. 9b and c shows phenol and TOC conversion as a function of time on stream in consecutive oxidation runs performed at different reaction temperatures in the presence of Ru(1.5 wt.%)/TiO_2 or Ru(3.0 wt.%)/TiO_2 catalysts. The effect of temperature was investigated in the range of 433–493 K, and the residence time of the liquid phase was about 0.14–0.16 min. The TOC removal was significantly improved as compared to runs conducted in the presence of TiO_2 support (Fig. 9a). It can be seen that temperature considerably affects the extent of TOC reduction and phenol

conversion. Under experimental conditions investigated, a decrease of catalyst activity was observed at temperatures ≤453 K over both catalysts. For example, the TOC removal decreased from 98 to 90% after 8 h (T = 453 K) and from 80 to 41% after 28 h of reaction (T = 433 K) (Fig. 9b). Simultaneously, a change of color from light yellow to dark brown in the outlet liquid phase was observed that was accompanied with the foam formation. The decrease of TOC with time on stream at constant temperature was not only due to partial oxidation of the surface of ruthenium particles (Fig. 2a, run #10: about 25% of Ru^0 undergoes oxidation), but was particularly due to strong adsorption of intermediates formed during the oxidative treatment. The color change of the outlet liquid phase demonstrated the formation of C-6 intermediate compounds, like benzoquinones and hydroquinones, which was also confirmed by HPLC analysis. A small increase in TOC removal observed in the subsequent oxidative step after increasing temperature from 433 to 453 K, might be attributed to partial reactivation of the catalyst. However, the TOC reduction was significantly improved above 453 K, which is attributed to considerable desorption and destruction of C-6 intermediates previously accumulated on the catalyst surface. For instance, TOC conversion increases from 40% at t = 50 h to 85% at 60 h with an increase of temperature from 453 to 473 K. It is evident from Fig. 9b that after reaching 473 K, a period of about 10 h is required to achieve stable catalyst activity with regard to TOC conversion. This confirms that desorption of C-6 intermediates from the catalyst surface is a temperature-activated process. After this period the Ru(1.5 wt.%)/TiO_2 catalyst exhibits stable activity (85% TOC removal, 95% phenol conversion), which together with the produced decolorized liquid phase indicates that intermediate products formed in the preceding oxidation steps were desorbed and transformed to carbon dioxide. In the off-gas stream, no carbon monoxide was detected. To avoid the formation of intermediates during phenol oxidation, CWAO experiments should be carried out at $T \geq 473$ K, which is clearly evident from Fig. 9b. It can be seen that by increasing temperature further to 493 K, total conversion of phenol was attained and only traces of organic carbon (98% TOC removal) remained in the liquid phase after ~80 h of reaction. The residual TOC was in the form of acetic acid, known to be particularly resistant to oxidation [20]. The carbon analysis performed at the end of run #10 revealed no differences between the fresh and used Ru(1.5 wt.%)/TiO_2 catalyst (Table 3). There is no deposition of carbon polymers, which can be produced by oxidative coupling reactions on the catalyst.

In an oxidation run presented in Fig. 9c (run #11), a decrease with time on stream in the activity of Ru(3.0 wt.%)/TiO_2 catalyst for TOC removal from phenol aqueous solution at 453 K was observed. According to the above discussion, it might be proposed again that the decrease of activity of the Ru(3.0 wt.%)/TiO_2 catalyst was mostly due to strong adsorption of partially oxidized C-6 intermediate products on the catalyst surface. As expected, upon increasing the reaction temperature to 483 or 493 K in subsequent oxidation steps, TOC removal and phenol conversion increased. Phenol is completely converted at 483 K and the obtained TOC removal is higher than 99%. It may also be noted that the activity of Ru(3.0 wt.%)/TiO_2 catalyst is constant during each oxidation step when $T \geq 473$ K (Fig. 9c). In this run, the amount of carbon deposited on the surface of catalyst particles was found to be 100 μg/g, which indicates that no accumulation of carbonaceous deposits took place on the surface of Ru(3.0 wt.%)/TiO_2 catalyst (Table 3, run #11).

Activity measurements coupled with the physicochemical characterization of spent catalysts after CWAO of acetic acid and phenol (Table 3 and Fig. 2) indicate that partial oxidation of Ru particles is not a prevailing factor in controlling the activity of catalysts during the CWAO of phenol (Fig. 9) because at conditions at which catalyst performance is not influenced by the adsorption of aromatic intermediates on the catalyst surface, constant phenol and TOC concentrations as a function of time on stream were obtained (Fig. 9b, ranges IV and V; Fig. 9c, ranges II, III and IV). On the other hand, the formation of RuO_2 on the catalyst surface has significant negative effect on the activity of Ru/TiO_2 catalysts during the CWAO of acetic acid (Fig. 7). These observations imply that very small amounts of acetic acid are accumulated in the liquid phase of CWAO of phenol carried out in the presence of Ru/TiO_2 catalysts. In other words, deep oxidation of phenol to CO_2 and H_2O undergoes oxidation routes, which do not result in significant formation of this refractory intermediate.

3.4. Acute toxicity of solutions

The calculated EC_{50} values, bioassay concentrations, end-product enhancement factors and detoxification factors for original and end-product solutions of CWAO are listed in Tables 4 and 5. It should be mentioned that in the case of *Vibrio fischeri* test (Table 4), the listed 30-min EC_{50} values for feed solutions of formic acid and acetic acid are similar to corresponding 30-min EC_{50} data reported by Santos et al. [43]. However, it was found out in this study that the exhibited toxic effect of these two compounds to *V. fischeri* is mostly due to low pH values of examined solutions (c_{feed} = 2.0 g/l) at test conditions, resulting from the dissociation of these compounds in water. The luminescence of *V. fischeri* is highly affected by pH changes as the 26% inhibition of luminescence was measured when the pH decreased from 7.0 to 6.5. When the solutions were neutralized to

Table 4
Toxicity to *Vibrio fischeri* of feed and end-product solutions of wet-air oxidation experiments carried out in the presence of TiO_2 and Ru/TiO_2 catalysts

Catalyst	Solution	30-min EC_{50} for feed solutions (95% CI) (mg/l)[a]	30-min EC_{50} for end products (95% CI) (vol.%)	Bioassay conc. of compounds in end product (mg/l)	End-product enhancement factor	% Detoxification	Detoxification factor	% TOC removal
TiO_2	Phenol, feed	22.3 (21.9–22.6)						
	Run #3a (493 K)		1.77 (1.60–1.94)	1260.0	1.9	−40.0	0.7	26.8
	Run #3a (513 K)		1.83 (1.72–1.95)	1218.6	2.4	−35.4	0.7	43.2
Ru(1.5 wt.%)/TiO_2	Formic acid, feed	59.0 (35.5–81.9)						
	Run #4 (383 K)		>100	<59	<14.3	>90.0	>10	99.3
Ru(3.0 wt.%)/TiO_2	Acetic acid, feed	108.8 (107.2–110.4)						
	Run #8 (503 K)		46.9 (46.7–47.0)	232.0	9.3	74.0	3.9	97.2
Ru(3.0 wt.%)/TiO_2	Phenol, feed	26.8 (26.0–27.6)						
	Run #11 (483 K)		22.3 (22.2–22.4)	120.2	13.8	87.6	8.1	99.1
	Run #11 (493 K)		61.1 (60.9–61.3)	43.9	7.6	95.5	22.2	99.4

[a] Expressed as mg/l TOC.

Table 5
Toxicity to *Daphnia magna* of feed and end-product solutions of wet-air oxidation experiments carried out in the presence of TiO_2 and Ru/TiO_2 catalysts

Catalyst	Solution	48-h EC_{50} for feed solutions (95% CI) (mg/l)[a]	48-h EC_{50} for end products (95% CI) (vol.%)	Bioassay conc. of compounds in end product (mg/l)	End-product enhancement factor	% Detoxification	Detoxification factor	% TOC removal
TiO_2	Phenol, feed	3.45 (2.45–4.67)						
	Run #3a (493 K)		1.1 (0.87–1.30)	313.6	0.5	65.2	2.9	26.8
	Run #3a (513 K)		1.5 (1.30–1.80)	230.0	0.5	74.4	3.9	43.2
Ru(1.5 wt.%)/TiO_2	Formic acid, feed	8.35 (7.83–8.35)						
	Run #4 (383 K)		67.1 (61.4–70.0)	12.4	3.0	97.9	41.7	99.3
Ru(3.0 wt.%)/TiO_2	Acetic acid, feed	19.2 (18.4–20.0)						
	Run #8 (503 K)		17.2 (13.2–18.7)	111.6	4.5	87.5	8.0	97.2
Ru(3.0 wt.%)/TiO_2	Phenol, feed	3.22 (2.37–4.37)						
	Run #11 (483 K)		18.5 (16.7–21.6)	17.4	2.0	98.2	55.6	99.1
	Run #11 (493 K)		21.6 (19.2–23.6)	14.9	2.6	98.5	66.7	99.4

[a] Expressed as mg/l TOC.

corresponding pH values prescribed by the standard procedure, the toxicity of both acids significantly decreased as the 45% inhibition of luminescence was found in the highest tested concentration (80 v/v, % of examined feed streams). In the case of *Daphnia magna* test (Table 5), the reported 48-h EC_{50} values for formic acid and acetic acid are in good agreement with the literature data [28,44–47]. It was further confirmed that they are not influenced by low pH values of acidic feed solutions, because the pH values of the tested concentrations, which were used to establish the 48-h EC_{50} values, were within the limits tolerable for aquatic organisms [48].

Comparison of the bioassay concentrations obtained by means of *V. fischeri* (Table 4), with the corresponding final TOC concentrations, indicates that in all cases the bioassay concentration was greater than the measured final TOC concentration. The same comparison performed for *D. magna* microcrustacean (Table 5) shows that in four out of the six experiments, the bioassay concentration was greater than the corresponding TOC concentration, especially during the CWAO of acetic acid. Accordingly, enhancement factors were greater than unity in these samples. This shows that the *V. fischeri* and *D. magna* reacted as if the end-product solution contained more than the known residual carbon content. The discrepancies between TOC measurements and bioassays could be attributed to the fact that the acute toxicity to *V. fischeri* and *D. magna* does not decrease proportionally to the extent of TOC removal. As discussed in the previous session, acetic acid was the only organic constituent of end-product solutions produced during the oxidative treatment of aqueous phenol stream. Therefore, by comparing results of runs #8 and 11 in Table 5, showing toxicity data for CWAO of acetic acid and phenol, respectively, one can see that 48-h EC_{50} values progressively increase with an increase of TOC conversion.

The values of % detoxification in Table 4 indicate that WAO of phenol feed solution over metal-free TiO_2 support resulted in the formation of end-product solution more toxic to *V. fischeri* than the original feed solution, although the TOC concentration decreased markedly. It is believed that this is due to the production and accumulation of partially oxidized C-6 intermediates (i.e. hydroquinones, benzoquinones) and higher molecular weight carboxylic and dicarboxylic acids in the liquid phase, which appear to be more toxic than the parent organic compound. On the other hand, this end-product solution was found to be less toxic to *D. magna* than the reactor feed stream (see Table 5). Furthermore, the same treatment carried out in the presence of Ru/TiO_2 catalysts appreciably reduced the toxicity of model solutions to both *V. fischeri* and *D. magna*. Calculated detoxification factors obtained in the presence of titania-supported Ru catalysts in the trickle-bed reactor are given in Table 4 and range from 3.9 to 22.2, meaning that the initial solutions were 3.9–22.2 more toxic to *V. fischeri* than the same solutions following CWAO. In the case of toxicity tests performed by *D. magna*, the detoxification factors were found to be in the range from 8.0 to 66.7 (Table 5). Considering low residence time of liquid phase in the catalytic bed (Fig. 3), the results of acute toxicity tests show great potential of employed Ru/TiO_2 catalysts for the detoxification of treated solutions of formic acid, acetic acid and phenol by means of CWAO technique. For example, acute toxicity to *D. magna* of aqueous phenol solution treated by the CWAO process was reduced by more than 98% (Table 5); for comparison, this value was higher than 95% in the case of *V. fischeri* test (Table 4). Although the acute toxicity to *D. magna* of phenol was greatly reduced, a comparison of results of 24-h (not shown) and 48-h EC_{50} tests confirms that there still exists some minor influence of CWAO end-product solutions on the mobility of test organisms.

The two aquatic organisms used in the performed acute toxicity measurements, the marine bacterium *V. fischeri* and the freshwater invertebrate *D. magna* clearly indicated that the toxicity diminished during the CWAO treatment especially when the Ru/TiO_2 catalysts were used. The *Vibrio fischeri* test provided lower % detoxification values and detoxification factors in this study in comparison to *D. magna*.

4. Conclusions

The reaction temperature, chemical potentials (partial pressures) of reactants and residence time affect the activity of Ru/TiO_2 catalysts and the toxicity of effluents resulting from CWAO of aqueous solutions of formic acid, acetic acid and phenol.

During CWAO runs the active Ru^0, which is supported over TiO_2 crystallites, partially oxidizes to RuO_2. The latter can be detected by H_2-TPR analysis of catalysts examined after the oxidation runs. This reveals that the CWAO process is accompanied by the simultaneous formation of RuO_2 species.

The TiO_2 support is active in TOC removal during the WAO of formic acid at conditions of $T \geq 373$ K and 10.0 bar of oxygen. Ru(1.5 wt.%)/TiO_2 and Ru(3.0 wt.%)/TiO_2 catalysts yielded complete removal of TOC at $T = 383$ K. Formation of partially oxidized Ru surface layer during the CWAO of formic acid seems not to affect the catalyst activity. Ru/TiO_2 promotes thermally induced decarboxylation of formic acid. The results of catalytic tests coupled with the physicochemical characterization of used catalysts after CWAO of acetic acid reveal that decrease of catalytic activity is due to partial oxidation of metallic ruthenium particles to RuO_2. For a given composition of the reaction mixture, the amounts of RuO_2 and Ru^0 depend on reaction temperature and concentration of liquid-dissolved O_2. Over 95% TOC reduction could be achieved in

the presence of Ru(3.0 wt.%)/TiO_2 catalyst at conditions of 503 K, 10.0 bar of oxygen and residence time of 0.14 min. Ru/TiO_2 catalysts are active for total conversion of phenol in aqueous solution at $T \geq 483$ K and 10.0 bar of oxygen partial pressure. The TOC abatement is greater than 99%; the rest of carbon is found in the form of acetic acid. At lower reaction temperatures ($T < 463$ K), adsorption of partially oxidized C-6 intermediates takes place on the catalyst surface, which results in apparent deactivation of Ru/TiO_2 catalysts. This can be avoided by conducting the CWAO process at sufficiently high temperatures which facilitate desorption of intermediates and their transformation to CO_2.

In the presence of Ru/TiO_2 catalysts, the acute toxicity to *D. magna* and *V. fischeri* of the oxidized materials was greatly reduced compared with that of the feed solutions. However, end-product solutions are generally more toxic than indicated by the concentrations of total organic carbon remaining in the reactor outlet streams. Before discharging them to the environment, evaluations of the residual toxicity should be performed that are based on actual bioassays, and not only on the potential of the CWAO process for destroying the original material entering the process.

Acknowledgement

The authors gratefully acknowledge the financial support of the Ministry of Education, Science and Technology of the Republic of Slovenia through Research program No. P2-0152.

References

[1] F. Luck, Catal. Today 53 (1999) 81.
[2] A. Cybulski, Ind. Eng. Chem. Res. 46 (2007) 4007.
[3] A. Cybulski, J. Trawczyński, Appl. Catal. B 47 (2004) 1.
[4] M. Abecassis-Wolfovich, M.V. Landau, A. Brenner, M. Herskowitz, J. Catal. 247 (2007) 201.
[5] N. Li, C. Descorme, M. Besson, Appl. Catal. B 76 (2007) 92.
[6] D. Duprez, F. Delanoë, J. Barbier Jr., P. Isnard, G. Blanchard, Catal. Today 29 (1996) 317.
[7] J.C. Béziat, M. Besson, P. Gallezot, S. Durécu, J. Catal. 182 (1999) 129.
[8] J.C. Béziat, M. Besson, P. Gallezot, S. Durécu, Ind. Eng. Chem. Res. 38 (1999) 1310.
[9] P.D. Vaidya, V.V. Mahajani, Chem. Eng. J. 87 (2002) 403.
[10] Y. Kojima, T. Fukuta, T. Yamada, M.S. Onyango, E.C. Bernardo, H. Matsuda, K. Yagishita, Water Res. 39 (2005) 29.
[11] N. Perkas, D. Pham Minh, P. Gallezot, A. Gedanken, M. Besson, Appl. Catal. B 59 (2005) 121.
[12] N. Li, C. Descorme, M. Besson, Appl. Catal. B 71 (2007) 262.
[13] D. Pham Minh, G. Aubert, P. Gallezot, M. Besson, Appl. Catal. B 73 (2007) 236.
[14] A. Pintar, M. Besson, P. Gallezot, Appl. Catal. B 30 (2001) 123.
[15] A. Pintar, M. Besson, P. Gallezot, Appl. Catal. B 31 (2001) 275.
[16] D. Pham Minh, P. Gallezot, M. Besson, Appl. Catal. B 75 (2007) 71.
[17] J. Wang, W. Zhu, S. Yang, W. Wang, Y. Zhou, Appl. Catal. B 78 (2008) 30.
[18] J. Levec, A. Pintar, Catal. Today 24 (1995) 51.
[19] L. Oliviero, J. Barbier Jr., D. Duprez, H. Wahyu, J.W. Ponton, I.S. Matcalfe, D. Mantzavinos, Appl. Catal. B 35 (2001) 1.
[20] J. Barbier Jr., F. Delanoë, F. Jabouille, D. Duprez, G. Blanchard, P. Isnard, J. Catal. 177 (1998) 378.
[21] J. Mikulová, S. Rossignol, J. Barbier Jr., D. Mesnard, C. Kappenstein, D. Duprez, Appl. Catal. B 72 (2007) 1.
[22] X. Shen, L.-J. Garces, Y. Ding, K. Laubernds, R.P. Zerger, M. Aindow, E.J. Neth, S.L. Suib, Appl. Catal. A 335 (2008) 187.
[23] Water quality – Determination of the inhibitory effect of water samples on the light emission of *Vibrio fischeri* (Luminescent bacteria test) – Part 2: Method using liquid-dried bacteria. ISO Standard No. 11348-2. ISO, Geneve, 1998.
[24] Dr. Lange LUMISsoft 4 software, Version 1.001, Düsseldorf, 2000.
[25] R. Kühn, M. Pattard, K.D. Pernack, A. Winter, Water Res. 23 (1984) 501.
[26] Water quality – Determination of the inhibition of the mobility of *Daphnia magna* Straus (Cladocera, Crustacea). ISO Standard No. 6341. ISO, Geneve, 1996.
[27] US Environmental Protection Agency toxicity data analysis software. EPA, Environmental Monitoring Systems Laboratory, Cincinnati (OH), 1994.
[28] R. Keen, C.R. Baillod, Water Res. 19 (1985) 767.
[29] G.C. Bond, R.R. Rajaram, R. Burch, Appl. Catal. 27 (1986) 379.
[30] G.C. Bond, R.R. Rajaram, R. Burch, J. Phys. Chem. 90 (1986) 4877.
[31] M.C.J. Bradford, M.A. Vannice, J. Catal. 183 (1999) 69.
[32] G.L. Haller, D.E. Resasco, Adv. Catal. 36 (1989) 173.
[33] R.T. Sanderson, in: H.H. Sisler, C.A. VanderWerf (Eds.), Inorganic Chemistry, Reinhold, New York, 1967, p. 204.
[34] P.G.J. Koopmann, A.P.G. Kieboom, H. Van Bekkum, J. Catal. 69 (1981) 172.
[35] F. Pinna, M. Signoretto, G. Strukul, A. Benedetti, M. Melentacchi, J. Catal. 155 (1995) 166.
[36] P. Betancourt, A. Rives, R. Hubaut, C.E. Scott, J. Goldwasser, Appl. Catal. A 170 (1998) 307.
[37] A. Lakota, J. Levec, AIChE J. 36 (1990) 1444.
[38] W.J.A. Wammes, K.R. Westerterp, Chem. Eng. Sci. 45 (1990) 2247.
[39] S. Goto, J.M. Smith, AIChE J. 21 (1975) 706.
[40] C.N. Satterfield, AIChE J. 21 (1975) 209.
[41] J.L.S. Bell, D.A. Palmer, H.L. Barnes, S.E. Drummond, Geochim. Cosmochim. Acta 58 (1994) 4155.
[42] T.M. McCollom, J.S. Seewald, Geochim. Cosmochim. Acta 67 (2003) 3645.
[43] A. Santos, P. Yustos, A. Quintanilla, F. Garcia-Ochoa, J.A. Casas, J.J. Rodriguez, Environ. Sci. Technol. 38 (2004) 133.
[44] G.P. Genoni, Ecotoxicol. Environ. Saf. 36 (1997) 27.
[45] Material Safety Data Sheet. https://fscimage.fishersci.com/msds/45433.htm (accessed December 2007).
[46] Material Safety Data Sheet. http://piercenet.com/files/EN1262.pdf (accessed December 2007).
[47] C.R. Janssen, E.Q. Espiritu, G. Persoone, in: A.M.V.M. Soares, P. Calow (Eds.), Progress in Standardization of Aquatic Toxicity Tests, Lewis Publishers, Boca Raton, 1993.
[48] Water quality – Sampling – Part 16: Guidance on biotesting of samples. ISO Standard No. 5667-16. ISO, Geneve, 1998.